A structural model for the yeast endonuclease is proposed in the accompanying report (8). A central feature of the model is represented by the strong Sen2-Sen54 and Sen34-Sen15 interactions that were detected with the two-hybrid system (9). The two dimers are associated to form a tetramer by way of the L10 loop sequences of Sen15 and Sen54. This model implies that Archaea and Eukaryotes have inherited from their common ancestor the endonuclease active sites and the means to array them in a precise and conserved spatial orientation. Our results with the artificial pre-tRNA$^{\text{Archeuka}}\left(\begin{smallmatrix}\text{U·A}\\ \text{G·C}\end{smallmatrix}\right)_{\nabla}$ and mini-BHB substrates strongly support that model.

REFERENCES AND NOTES

1. M. Belfort and A. Weiner, *Cell* **89**, 1003 (1997).
2. V. M. Reyes and J. Abelson, *Ibid.* **55**, 719 (1988).
3. E. Mattoccia, M. I. Baldi, D. Gandini Attardi, S. Ciafrè, G. P. Tocchini-Valentini, *ibid.*, p. 731.
4. L. D. Thompson and C. J. Daniels, *J. Biol. Chem.* **265**, 18104 (1990).
5. M. I. Baldi, E. Mattoccia, E. Bufardeci, S. Fabbri, G. P. Tocchini-Valentini, *Science* **255**, 1404 (1992).
6. S. Fabbri *et al.*, data not shown.
7. E. Di Nicola Negri *et al.*, *Cell* **89**, 859 (1997).
8. H. Li, C. R. Trotta, J. Abelson, *Science* **280**, 279 (1998).
9. C. R. Trotta *et al.*, *Cell* **89**, 849 (1997).
10. D. Gandini Attardi, M. I. Baldi, E. Mattoccia, G. P. Tocchini-Valentini, *Methods Enzymol.* **181**, 510 (1989).
11. L. D. Thompson and C. J. Daniels, *J. Biol. Chem.* **263**, 1751 (1988).
12. Pre-tRNA$^{\text{Phe}}$ and pre-tRNA$^{\text{Phe}}\left(\begin{smallmatrix}\text{U·A}\\ \text{G·C}\end{smallmatrix}\right)_{\nabla}$ were synthesized as described (*3*, *5*, *7*). Templates for the synthesis of the Archaeuka precursors were constructed by polymerase chain reaction (PCR). The PCR templates were the full-length pre-tRNAs. One primer contained the T7 promoter and part of the 5′ exon. The other was composed of the desired sequence of the 3′ exon. Conditions for PCR, transcription by T7 RNA polymerase, and endonuclease assays were as described (*3*, *5*, *7*). *Xenopus laevis* endonuclease was purified as in (*10*), *Saccharomices cerevisiae* endonuclease as in (*9*), and *S. sulfataricus* endonuclease as in (*11*).

13. We thank J. Dahlberg for help with the manuscript; J. Abelson for helpful comments, for communicating results before publication, and for yeast endonuclease; R. H. Haselkorn for critical reading of the manuscript; M. Rossi for *S. sulfataricus* cells; G. Di Franco for technical assistance; and A. Sebastiano for typesetting help with the manuscript. Supported in part by Progetto Finalizzato (CNR) Ingegneria Genetica, Progetto Finalizzato (CNR) Biotecnologie, Human Frontiers Science Program Organization (HFSPO), and Fondo Cinquepercento: Biotecnologie.

15 December 1997; accepted 9 February 1998

Ribosome-Catalyzed Peptide-Bond Formation with an A-Site Substrate Covalently Linked to 23S Ribosomal RNA

Rachel Green,* Christopher Switzer, Harry F. Noller†

In the ribosome, the aminoacyl–transfer RNA (tRNA) analog 4-thio-dT-p-C-p-puromycin crosslinks photochemically with G2553 of 23S ribosomal RNA (rRNA). This covalently linked substrate reacts with a peptidyl-tRNA analog to form a peptide bond in a peptidyl transferase–catalyzed reaction. This result places the conserved 2555 loop of 23S rRNA at the peptidyl transferase A site and suggests that peptide bond formation can occur uncoupled from movement of the A-site tRNA. Crosslink formation depends on occupancy of the P site by a tRNA carrying an intact CCA acceptor end, indicating that peptidyl-tRNA, directly or indirectly, helps to create the peptidyl transferase A site.

Catalysis of peptide bond formation requires precise juxtaposition of the acceptor ends of P (peptidyl)- and A (aminoacyl)-site–bound tRNAs in the active site of the ribosome. Accumulating evidence points to a role for the 23S rRNA in the function of peptidyl transferase (*1*–*3*). Identification of a peptidyl transferase–reactive crosslink between a benzophenone-derivatized peptidyl-tRNA and A2451-C2452 localized the central loop of domain V of 23S rRNA to the peptidyl transferase site (*2*). More recently, identification of a base-pairing interaction between C74 of P-site–bound tRNA and G2252 of domain V established a direct role for 23S rRNA in the function of peptidyl transferase (*3*). Here we describe an aminoacyl-tRNA analog, 4-thio-dT-p-C-p-puromycin (s^{4}TCPm), which crosslinks to 23S rRNA with high efficiency and specificity. This substrate remains fully active as an acceptor in the peptidyl transferase reaction while covalently bound to 23S rRNA, imposing constraints on the proposed concerted events of tRNA movement and peptide-bond formation and unambiguously placing the conserved 2555 loop of 23S rRNA at the peptidyl transferase A site.

The aminoacyl-tRNA analog, s^{4}TCPm, was chemically synthesized and purified (*4*); the Michaelis constant (K_m) of this compound for peptidyl transferase is about 10 μM (*5*). The phosphorylated compound, [^{32}P]s^{4}TCPm, was then bound to *Escherichia coli* 70S ribosomes programmed with gene *32* mRNA (*6*) in which the P site was filled with deacylated tRNA$^{\text{Phe}}$. After irradiation with ultraviolet (UV) light (366 nm), total RNA was prepared from the ribosomal complexes and analyzed (Fig. 1A) (*7*). Exclusive labeling of 23S rRNA is consistent with crosslinking to the peptidyl transferase center of the ribosome. Based on incorporation of ^{32}P into 23S rRNA, about 30% of ribosomes were crosslinked in the presence of 20 μM s^{4}TCPm. The absence of substantial crosslinking to ribosomal proteins (*8*) provides evidence for the specificity of the crosslinked A-site ribosomal complex and the RNA-rich nature of the peptidyl transferase site (*9*). This contrasts with the recent proposal of a proteinaceous A-site environment (*10*).

Digestion of the crosslinked *E. coli* 23S rRNA species with ribonuclease (RNase) T1 (*11*) revealed a single crosslinked product (Fig. 1B). The efficiency and specificity of crosslinking was high, which indicates an extremely close juxtaposition of s^{4}TCPm and rRNA, comparable to that between position 34 of tRNA and position C1400 of 16S rRNA (*12*). Typically, even highly efficient crosslinks to the ribosome, such as those obtained with benzophenone-derivatized Phe-tRNA$^{\text{Phe}}$, target multiple rRNA sites (*2*).

Assignment of the site of crosslinking to position G2553 was achieved with RNase H digestion (*13*) followed by primer-extension analysis (Fig. 1C) (*14*). The strong stop induced by crosslinking with s^{4}TCPm is consistent with the estimated crosslinking efficiency of 30%. Crosslinking of s^{4}TCPm to *Bacillus stearothermophilus* ribosomes was similarly efficient and also yielded a single RNase T1 product; primer extension again localized the crosslinked position to nucleotide G2553 (*E. coli* numbering) (*8*).

The crosslink between s^{4}TCPm and 23S rRNA places the conserved 2555 loop at the site of interaction between the ribosome and the conserved CCA end of A-site tRNA. This conclusion is consistent with protection of G2553 from chemical modification by A-site tRNA, which depends on the presence of the terminal adenosine (A76) of tRNA (*15*) and with directed cleavage of this region of the RNA backbone by hydroxyl radicals generated from Fe(II) tethered to the 5′ end of A-site–

R. Green and H. F. Noller, Center for Molecular Biology of RNA, Sinsheimer Laboratories, University of California, Santa Cruz, CA 95064, USA.
C. Switzer, Department of Chemistry, University of California, Riverside, CA 92521, USA.

*Present address: Department of Molecular Biology and Genetics, Johns Hopkins University School of Medicine, Baltimore, MD 21205, USA.
†To whom correspondence should be addressed. E-mail: harry@nuvolari.ucsc.edu

bound tRNA (*16*). Other biochemical and genetic experiments are similarly consistent (*17*). Both G2553 and Um2552 are universally conserved nucleotides, suggesting possible interactions between these nucleotides of 23*S* rRNA and the similarly conserved CCA end of A-site–bound tRNA.

Crosslinked *E. coli* 50*S* subunit–s^4TCPm complexes were isolated and tested for the ability of the covalently bound A-site substrate to participate in peptide bond formation (*18*). The minimal P-site oligonucleotide substrate CACCA-(*N*-Ac-Phe) was supplied and its reaction with the crosslinked puromycin complex was followed by a shift in the electrophoretic mobility of the RNase T1 fragment of 23*S* rRNA resulting from acquisition of *N*-Ac-Phe [resulting product, *N*-Ac-Phe-(s^4TCPm)-23*S* T1 oligonucleotide] (Fig. 2A). The rate of reaction of the covalently bound substrate is similar to that observed in a standard reaction with 50*S* subunits in which free puromycin is supplied at a saturating concentration. Crosslinked *B. stearothermophilus* 50*S*–s^4TCPm complexes were also reactive in a peptidyl transferase reaction (*8*). Thus, the A-site substrate s^4TCPm is crosslinked to 23*S* rRNA in its biologically active configuration.

A number of peptidyl transferase–specific antibiotics, including chloramphenicol, carbomycin, clindamycin, sparsomycin, and puromycin, specifically inhibited the crosslinking of s^4TCPm to the 2555 loop of 23*S* rRNA; erythromycin and neomycin, two antibiotics that do not target peptidyl transferase, had no effect (Fig. 2B) (*19*). However, only chloramphenicol, carbomycin, and clindamycin strongly inhibited the peptidyl transferase reactivity of the crosslinked complex (Fig. 2C) (*19*). Sparsomycin and puromycin, both known to directly compete with aminoacyl-tRNA binding to the A site, predictably had no effect on the peptidyl transferase activity of the crosslinked complex (*20*, *21*). These effects provide further evidence that the synthetic substrate, s^4TCPm, is crosslinked to its physiologically correct binding site.

Crosslinking of s^4TCPm is strongly dependent on occupancy of the P site with deacylated $tRNA^{Phe}$ (Fig. 3A). To determine which particular features of P-site tRNA are required for binding to the A site, we constructed several mutant versions of $tRNA^{Phe}$ containing alterations of the CCA terminus (*22*). None of the altered tRNAs, when bound to the P site, was able to support efficient crosslinking of s^4TCPm in the A site (Fig. 3A). Requirement for a specific Watson-Crick interaction in the P site between C74 of tRNA and G2252 of 23*S* rRNA (*3*) was demonstrated by the inability of C74A mutant tRNA to stimulate efficient A-site s^4TCPm crosslinking except in the context of G2252U mutant ribosomes (Fig. 3B). A properly engaged, intact P-site–bound tRNA is required for formation of this highly efficient A-site crosslink. Thus, the A site on the 50*S* subunit may be incompletely formed (or is inaccessible) in the absence of P-site–bound tRNA or the P-site tRNA itself provides one or more of the A-site binding determinants. Cooperative interactions between P-site– and A-site–bound tRNAs have been reported (*21*, *23*).

Our findings have strong implications for the displacement and hybrid state (*24*) models for the movements of tRNA substrates in the translational elongation cycle. Both models invoke coupling of the peptidyl transferase reaction with movement of the

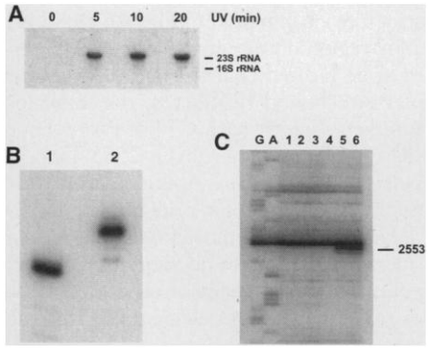

Fig. 1. Identification and localization of a crosslink between [^{32}P]s^4TCPm and 23*S* rRNA. (**A**) Ribosomal complexes (*7*) were exposed for various lengths of time to long wavelength (366 nm) UV light. Ribosomal RNAs were extracted with phenol and analyzed on a 3.8% polyacrylamide gel containing 7 M urea. (**B**) ^{32}P-radiolabeled A-site substrate [^{32}P]s^4TCPm (lane 1) and an RNase T1 digestion of crosslinked 23*S* rRNA resolved on a 24% polyacrylamide gel containing 6 M urea (lane 2) (*11*). (**C**) Primer extension analysis of crosslinked *E. coli* 23*S* rRNA. Lanes: G and A, sequencing lanes; 1 to 3, absence of s^4TCPm for 0, 5, and 15 min of exposure, respectively, to UV light; 4 to 6, presence of s^4TCPm for 0, 5 and 15 min of exposure, respectively, to UV light (*15*). The strong reverse transcriptase stop correlated with the presence of crosslinking reagent is indicated at G2553.

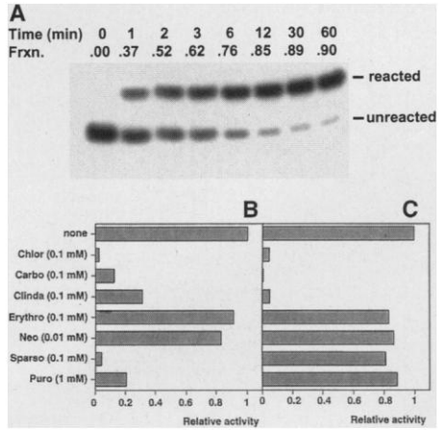

Fig. 2. Peptidyl transferase activity of the crosslinked s^4TCPm-50*S* complex. (**A**) Peptidyl transferase reactivity of s^4TCPm covalently bound to ribosomes with P-site substrate CACCA-(*N*-Ac-Phe). Reaction products were analyzed by RNase T1 digestion of 23*S* rRNA and resolved on a 24% polyacrylamide gel containing 6 M urea (*11*, *18*). The reaction time and extent of reaction (Frxn.) are indicated. (**B**) Antibiotic inhibition of crosslinking by s^4TCPm to 23*S* rRNA (*19*). Values were normalized to 1.0 for the reaction mixture with no antibiotics. (**C**) Antibiotic inhibition of peptidyl transferase activity of crosslinked complex (s^4TCPm-50*S*) (*19*). Values were normalized as in (B). Chlor, chloramphenicol; Carbo, carbomycin; Clinda, clindamycin; Erythro, erythromycin; Neo, neomycin; Sparso, sparsomycin; Puro, puromycin.

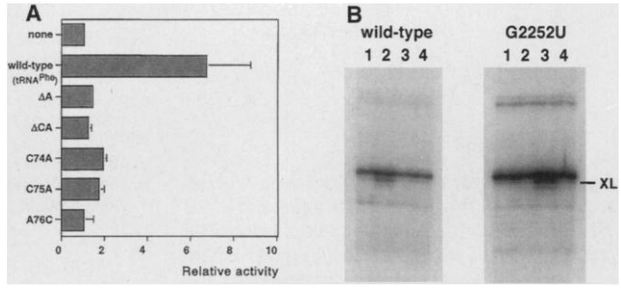

Fig. 3. Crosslinking of s^4TCPm to the A site of the ribosome depends on occupancy of the P site by an intact tRNA. (**A**) Analysis of $tRNA^{Phe}$ species with mutant CCA acceptor ends. Ribosomal complexes were formed (*7*) with the indicated alterations of the CCA acceptor end of deacylated $tRNA^{Phe}$ in the P site and limiting [^{32}P]s^4TCPm in the A site and exposed to UV light. Radioactivity incorporated into 23*S* rRNA was normalized to the amount incorporated in the absence of any $tRNA^{Phe}$. (**B**) Suppression of C74A $tRNA^{Phe}$ crosslinking deficiency with mutant ribosomes [G2252 to U (G2252U)]. Ribosomal complexes were formed with saturating s^4TCPm and various $tRNA^{Phe}$ species [lane 1, none; lane 2, wild type (CCA); lane 3, C74A (ACA); lane 4, C75A (CAA)] and exposed to UV light. Allele-specific primer extension (PSII) was used to compare the extent of 23*S* rRNA crosslinking in wild-type and G2252U mutant ribosomal populations (*3*).

acceptor end of A-site–bound tRNA into the P site of the 50S subunit. The efficient catalysis performed by the crosslinked complex suggests that either the crosslinked product retains sufficient mobility to undergo movement (which may be modest), that movement is coupled to intramolecular rearrangement of 23S rRNA, or that peptidyl transfer and movement are sequential rather than concerted.

The active site of the ribosome is thus composed of at least three distal elements of 23S rRNA dispersed across the secondary structure of domain V (Fig. 4): the 2451–2452 region of the central loop of domain V must be located near the aminoacyl moiety of P-site–bound tRNA (*2*), the 2250 loop interacts directly with C74 of P-site–bound tRNA (*3*), and, here, the 2555 loop has been localized to the A-site–bound tRNA. Such data argue for a primary role for 23S rRNA in peptidyl transferase and force consideration of the steric limitations on the potential involvement of other 23S rRNA or ribosomal protein elements in this catalytic site.

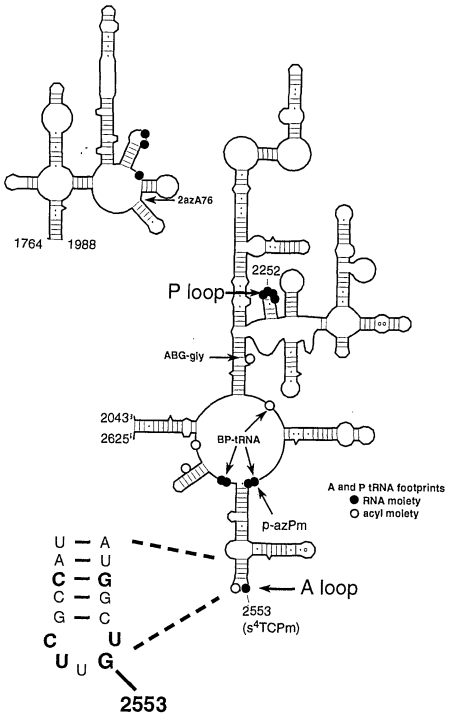

Fig. 4. Secondary structure of domains IV (part) and V of 23S rRNA. The footprints of A and P site tRNAs (closed circles for RNA-protected moieties and open circles for acyl-protected moieties) are indicated (*15*). Several sites crosslinked by the acceptor end of P- and A-site–bound tRNAs are indicated with small arrows (*29*). Two specific nucleotides, G2252 and G2553, known to form close contact with the CCA end of P- and A-site–bound tRNAs, respectively, are indicated; the loops in which these nucleotides are found are designated the P loop (*30*) and the A loop.

REFERENCES AND NOTES

1. K. R. Lieberman and A. E. Dahlberg, *Prog. Nucleic Acids Res. Mol. Biol.* **50**, 1 (1995); R. Green and H. F. Noller, *Annu. Rev. Biochem.* **66**, 679 (1997); H. F. Noller, V. Hoffarth, L. Zimniak, *Science* **256**, 1416 (1992).
2. G. Steiner, E. Kuechler, A. Barta, *EMBO J.* **7**, 3949 (1988); A. Barta, G. Steiner, J. Brosius, H. F. Noller, E. Kuechler, *Proc. Natl. Acad. Sci. U.S.A.* **81**, 3607 (1984).
3. R. R. Samaha, R. Green, H. F. Noller, *Nature* **377**, 309 (1995).
4. 5′-Dimethoxytrityl-N^{α}-trifluoroacetyl puromycin was attached to alkylamine-derivatized controlled pore glass via a 2′-succinate linkage by standard methods (*25*). s^4TCPm was prepared by standard phosphoramidite chemistry with the solid-phase version of puromycin and riboC and 4-thio-dT phosphoramidites (Glen Research). Deprotection was performed by treatment with 3:1 NH_4OH/MeOH containing 50 mM NaSH overnight at 55°C. Subsequently, 40 equivalents of 1 M tetrabutylammonium fluoride in tetrahydrofuran were added to the dried product and incubated overnight at room temperature. Finally, 20 mM triethylamine acetate (pH 7.0) was added to the reaction mixture, and it was loaded directly on a C_{18} high-performance liquid chromatography column and eluted with increasing concentrations of acetonitrile (CH_3CN). Products were collected and their purity was analyzed on a 20% polyacrylamide, 7 M urea gel after 5′ ^{32}P-end-labeling with polynucleotide kinase.
5. Kinetic characterization of s^4TCPm was done with the tRNA fragment *N*-Ac-Met-ACCACC used as a P-site substrate, under fragment reaction conditions (*18*), and with analysis of the resulting product s^4TCPm-*N*-Ac-Met by paper electrophoresis. The apparent K_m of this compound for the ribosome was 10 μM, although at high concentrations peptidyl transferase activity was inhibited (*8*). This is consistent with binding competition by s^4TCPm at the P site attributable to wobble pairing between 4-thio-dT (which mimics C74 of tRNA) and G2252 of 23S rRNA (*3*); no alternative crosslink associated with P-site occupation by s^4TCPm was observed.
6. D. Hartz, D. S. McPheeters, L. Gold, *Methods Enzymol.* **164**, 419 (1988).
7. Tight-couple *E. coli* 70S ribosomes (2 μM) were incubated with 1.2 equivalents (2.4 μM) of gene 32 mRNA (*6*) and deacylated $tRNA^{Phe}$ (*26*) in 20 mM tris (pH 7.5), 30 mM $MgCl_2$, 50 mM NH_4Cl, 6 mM 2-mercaptoethanol, and 10% MeOH. Saturating s^4TCPm (20 μM) (or [^{32}P]s^4TCPm) was then added and the mixture was incubated at 37°C for 10 min. s^4TCPm was crosslinked to *B. stearothermophilus* 70S ribosomes under similar conditions except 30 mM tris (pH 7.5) containing 10 mM $MgCl_2$ and 330 mM KCl was used. Complexes were exposed for various lengths of time to a hand-held UV light source (366 nm) (UVL-56, Blak-Ray Lamp, UVP) at a distance of 3 cm (*27*). The intact rRNAs were then extracted with phenol and resolved on 3.8% polyacrylamide gels containing 7 M urea.
8. R. Green and H. F. Noller, unpublished data.
9. W. D. Picking, O. W. Odom, B. Hardesty, *Biochemistry* **31**, 12565 (1992).
10. C. Rodriguez-Fonseca, R. Amils, R. A. Garrett, *J. Mol. Biol.* **247**, 224 (1995).
11. The ^{32}P-radiolabeled crosslinked 23S rRNA species was digested with RNase T1 in 0.2 M NaOAc (pH 5.5) containing 2.5 mM EDTA at 37°C for 20 min and the products were resolved on 24% polyacrylamide gels containing 6 M urea.
12. I. Schwartz and J. Ofengand, *Biochemistry* **17**, 2524 (1978); J. B. Prince, B. H. Taylor, D. L. Thurlow, J. Ofengand, R. A. Zimmerman, *Proc. Natl. Acad. Sci. U.S.A.* **79**, 5450 (1982).
13. O. Dontsova *et al.*, *EMBO J.* **11**, 3105 (1992); R. Green and H. F. Noller, *RNA* **2**, 1011 (1996).
14. Primer-extension analysis was performed on ribosomal complexes formed in the presence or absence of unlabeled s^4TCPm compound using cDNA 2639 (5′-CTAGGAGCAGCCCCCC-3′) (*15*).
15. D. Moazed and H. F. Noller, *Cell* **57**, 585 (1989).
16. S. Joseph and H. F. Noller, *EMBO J.* **15**, 910 (1996).
17. D. J. Eckermann and R. H. Symons, *Eur. J. Biochem.* **82**, 225 (1978); M. O'Connor and A. E. Dahlberg, *Proc. Natl. Acad. Sci. U.S.A.* **90**, 9214 (1993).
18. Crosslinked 50S subunits were separated from 30S subunits, gene *32* mRNA, and deacylated $tRNA^{Phe}$ on 5 to 20% sucrose gradients in 10 mM tris-HCl (pH 7.5), 30 mM NH_4Cl, and 1 mM $MgCl_2$ spun in an SW41 rotor at 19,000 rpm for 16 hours. Excess sucrose was removed and the buffer was exchanged to 20 mM tris (pH 7.5), 100 mM NH_4Cl, and 5 mM $MgCl_2$ using Centricon 100 tubes spun at 2600 revolutions per minute in an SS34 rotor. Peptidyl transferase assays were done as follows: crosslinked 50S subunit complexes (0.5 μM) were incubated under fragment reaction conditions [50 mM tris (pH 8.3), 0.4 M KOAc, 60 mM $MgCl_2$ and 33% MeOH] with CACCA-(*N*-Ac-Phe) (2 μM). Aliquots were removed from the reaction mixture at the indicated times, the rRNAs were extracted with phenol and digested with RNase T1, and the fragments were resolved on 24% polyacrylamide gels containing 6 M urea.
19. For inhibition analysis, antibiotics were added to the reaction mixture described above at the following concentrations: chloramphenicol, 0.1 mM; carbomycin, 0.1 mM; clindamycin, 0.1 mM; erythromycin, 0.1 mM; neomycin, 0.01 mM; sparsomycin, 0.1 mM; and puromycin, 1 mM. When incubated with ribosomes at these concentrations, the antibiotics protect specific positions in 16S and 23S rRNA from chemical modification (*28*). Antibiotic inhibition of crosslinking was performed with limiting [^{32}P]s^4TCPm and a single time point (2 min) of exposure to UV light (in the linear range of the reaction) under standard conditions. Antibiotic inhibition of peptidyl transferase activity was performed with the fragment P-site substrate, CACCA-(*N*-Ac-Phe), supplied at a concentration of 0.3 μM; a single linear time point of 4 min was used for analysis.
20. I. H. Goldberg and K. Mitsugi, *Biochemistry* **6**, 383 (1967).
21. S. Pestka, *Cold Spring Harbor Symp. Quant. Biol.* **34**, 395 (1969).
22. Templates for transcription of mutant $tRNA^{Phe}$ were generated by polymerase chain reaction amplification of CF23 plasmid (*26*) with the following primers; T7 top, 5′-TAA TAC GAC TCA CTA TAG-3′; ΔA, 5′-GGT GCC CGG ACT CGG AAT CGA-3′; ΔCA, 5′-GTG CCC GGA CTC GGA ATC GAA-3′; C74A, 5′-TGT TGC CCG GAC TCG GAA TCG-3′; C75A, 5′-TTG TGC CCG GAC TCG GAA TCG-3′; and A76C, 5′-GGG TGC CCG GAC TCG GAA TCG-3′. Amplified DNA was extracted once with phenol and once with chloroform, precipitated with ethanol, and transcribed in vitro with T7 RNA polymerase under standard conditions with the following alterations; 2 mM each nucleoside triphosphate, 10 mM guanosine 5′-monophosphate, and 14 mM $MgCl_2$. Crude transcription reaction mixtures were purified on 12% acrylamide gels (55 cm long, 1 mm thick) containing 7 M urea and with the xylene cyanol dye marker run to the bottom (*26*). Transcripts were passively eluted into 0.3 M NaOAc, extracted with phenol and chloroform, and precipitated. RNAs were then labeled with [^{32}P]*Cp* and T4 RNA ligase and digested to completion with 1 unit of RNase T2 in 100 mM NH_4OAc (pH 5.4) at 37°C for 120 min. Np (Ap, Cp, Gp, and Up) products were resolved by paper electrophoresis at pH 3.5 (pyridine acetate) (30 min at 3000 V). The integrity of the 3′ termini of the mutant tRNAs was at least 75% correct (*8*).
23. T. Hishizawa and S. Pestka, *Arch. Biochem. Biophys.* **147**, 624 (1971); B. Ulbrich, G. Mertens, K. H. Nierhaus, *ibid.* **190**, 149 (1978).
24. B. Hardesty, O. W. Odom, H.-Y. Deng, in *The Structure, Function and Genetics of Ribosomes*, B. Hardesty and G. Kramer, Eds. (Springer-Verlag, New York, 1986), pp. 495–508; D. Moazed and H. F. Noller, *Nature* **342**, 142 (1989).
25. T. Atkinson and M. Smith, in *Oligonucleotide Synthesis: A Practical Approach*, M. Gait, Ed. (IRL Press, Oxford, 1985), pp. 35–81.
26. J. R. Sampson and O. C. Uhlenbeck, *Proc. Natl. Acad. Sci. U.S.A.* **85**, 1033 (1988).
27. W. Tate, B. Greuer, R. Brimacombe, *Nucleic Acids Res.* **18**, 6537 (1990).

28. D. Moazed and H. F. Noller, *Nature* **327**, 389 (1987); *Biochimie* **69**, 879 (1987).
29. J. Wower, S. S. Hixson, R. A. Zimmerman, *Proc. Natl. Acad. Sci. U.S.A.* **86**, 5232 (1989); P. Mitchell, K. Stade, M. Osswald, R. Brimacombe, *Nucleic Acids Res.* **15**, 8783 (1993); C. C. Hall, D. Johnson, B. S. Cooperman, *Biochemistry* **27**, 3983 (1988); G. Steiner, E. Kuechler, A. Barta, *EMBO J.* **7**, 3949 (1988).
30. E. V. Puglisi, R. Green, H. F. Noller, J. D. Puglisi, *Nature Struct. Biol.* **4**, 775 (1997).
31. We thank B. Cormack, G. Culver, L. Holmberg, K. Fredrick, K. Lieberman, and E. Strauss for helpful comments on the manuscript and S. Joseph and C. Merryman for helpful discussions. Supported by grants from the National Institutes of Health, the National Science Foundation, the Lucille P. Markey Charitable Trust to the Center for Molecular Biology of RNA, and a Burroughs-Wellcome Career Award to R.G.

21 November 1997; accepted 10 February 1998

Visual Input to the Efferent Control System of a Fly's "Gyroscope"

Wai Pang Chan, Frederick Prete, Michael H. Dickinson*

Dipterous insects (the true flies) have a sophisticated pair of equilibrium organs called halteres that evolved from hind wings. The halteres are sensitive to Coriolis forces that result from angular rotations of the body and mediate corrective reflexes during flight. Like the aerodynamically functional fore wings, the halteres beat during flight and are equipped with their own set of control muscles. It is shown that motoneurons innervating muscles of the haltere receive strong excitatory input from directionally sensitive visual interneurons. Visually guided flight maneuvers of flies may be mediated in part by efferent modulation of hard-wired equilibrium reflexes.

Flies are among the most maneuverable of all flying animals and generate elaborate flight behaviors under visual control (*1*). For example, a male housefly initiates a corrective tracking maneuver within 30 ms of detecting a deviation in the flight trajectory of a female that it is chasing (*2*). Flies have several unique specializations that enable them to detect and respond to moving targets with such rapidity. These specializations include a visual system with a flicker fusion rate of 300 Hz (*3*) and wings capable of achieving an aerodynamic performance that is two to three times greater than that generated by conventional steady-state mechanisms (*4*). Perhaps the most remarkable specialization of the flight system of flies is the evolutionary transformation of the hind wings into equilibrium organs called halteres, tiny club-shaped organs that beat antiphase to the wings during flight (*5*). Although the halteres have lost their aerodynamic role through evolution, the sensory fields at their base have hypertrophied relative to their homologs at the base of the wings (*6*). In the blow fly *Calliphora vicina*, the haltere is equipped with about 335 strain-sensitive campaniform sensilla organized in five distinct fields on the haltere base (*7*). Sensory cells innervating a subpopulation of these sensilla encode Coriolis forces that result from the cross product of the haltere's linear velocity with the angular velocity of the fly's body around the yaw, pitch, or roll axes (*8*). Through their strong connections with steering motoneurons of the wing, the haltere afferents mediate stabilizing flight control reflexes (*9*, *10*). With their halteres removed, flies are unstable and quickly crash to the ground (*11*).

In many animals, efferent regulation modulates the sensitivity of sensory systems. In mammals, mechanical feedback mediated through efferent control of the outer hair cells within the cochlea is responsible for the sharp tuning of the primary auditory receptors (*12*). In vertebrate muscle spindles, fusimotor efferents can adjust the length of intrafusial fibers to set the sensitivity of the spindle sensory afferents (*13*). Similarly, in

W. P. Chan and M. H. Dickinson, Department of Integrative Biology, University of California, Berkeley, CA 94720, USA.
F. Prete, Department of Psychology, DePaul University, 1036 West Belden Avenue, Chicago, IL 60614, USA.
*To whom correspondence should be addressed.

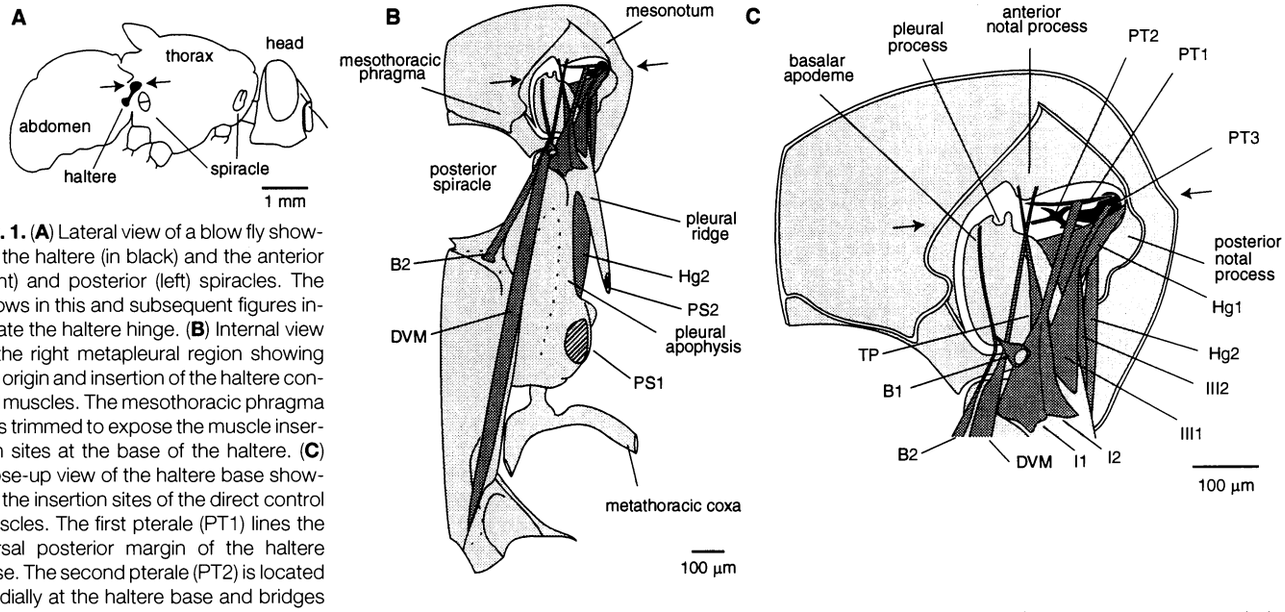

Fig. 1. (**A**) Lateral view of a blow fly showing the haltere (in black) and the anterior (right) and posterior (left) spiracles. The arrows in this and subsequent figures indicate the haltere hinge. (**B**) Internal view of the right metapleural region showing the origin and insertion of the haltere control muscles. The mesothoracic phragma was trimmed to expose the muscle insertion sites at the base of the haltere. (**C**) Close-up view of the haltere base showing the insertion sites of the direct control muscles. The first pterale (PT1) lines the dorsal posterior margin of the haltere base. The second pterale (PT2) is located medially at the haltere base and bridges the dorsal and ventral margin of the haltere's articulation with the metathorax. The third pterale (PT3) forms the posterior corner of the haltere base. The largest sclerite, the basalare, is fused to the pleural process and sits just anterior and ventral to the haltere. These four sclerites are surrounded anteriorly and dorsally by the anterior notal process, posteriorly by the posterior notal process, and ventrally by the pleural process.